Available online at www.sciencedirect.com

jmr&t Journal of Materials Research and Technology

journal homepage: www.elsevier.com/locate/jmrt

Original Article

# Characterization of coir fiber powder (*cocos nucifera L.*) as an environmentally friendly inhibitor pigment for organic coatings

*B.R. Freitas* [a,*], *J.O. Braga* [a], *M.P. Orlandi* [a], *B.P. da Silva* [b], *I.V. Aoki* [b], *V.F.C. Lins* [a], *F. Cotting* [a]

[a] *Universidade Federal de Minas Gerais - Graduate Program Chemical Engineering, Brazil*
[b] *Chemical Engineering Department of Polytechnic School of the University of São Paulo, Brazil*

ARTICLE INFO

*Article history:*
Received 29 March 2022
Accepted 14 May 2022
Available online 21 May 2022

*Keywords:*
Pigment inhibitor
Corrosion
Fiber coconut
Alkaline treatment
Agricultural waste

ABSTRACT

The reuse of an agricultural by-product in consense with the development of green coatings, motivated the characterization of coconut fiber powder, as a renewable inhibitor pigment. Coconut microfibers are a new, efficient, eco-friendly inhibitor pigment. The aim of this work to homogenize the particle size - MESH 250 -, the fiber was milled and sieved. The coconut fiber powder underwent an alkaline treatment, with immersion in sodium hydroxide solution - NaOH 5% (w/w) - for 24 h. The morphological characterization of untreated microfiber (UM) and treated microfiber (TM) were performed using laser diffraction and scanning electron microscopy (SEM). The compositions of the UM and TM samples were analyzed by Fourier Transform Infrared Spectroscopy (FTIR) and their thermal decomposition by the thermogravimetric analysis (TG/DG). The samples were characterized as a coating pigment in terms of density, oil absorption, and CPVC. Weight loss and potentiodynamic polarization curves tests were performed for understanding the inhibitory effect of fiber powder samples. Despite the high oil absorption of the samples (UM-95.73, TM-99.46) it has a low density, therefore presenting CPVC values that allow the formulation of coatings with ideal PVC. The FTIR showed that the untreated microfiber samples had lignocellulosic matrix and tannins in their composition, the treated sample showed removal of some materials from the structure, increasing the lignin concentration. The mass loss and potentiodynamic assays showed an inhibition efficiency of approximately 70% for UM and 90% for TM.



* Corresponding author.
E-mail address: barbara.rodrigues95@hotmail.com (B.R. Freitas).
https://doi.org/10.1016/j.jmrt.2022.05.098

## 1. Introduction

The fiber coconut is an agricultural waste with excellent chemical-physics proprieties, and it is produced on a large scale worldwide. The world production of coir approximately 18.7 million tons of fiber coconut are discarded [1]. However, coconut fibers are rich of lignocellulosic sources and couild may be used in a wide range of industrial applications. These fibers can be obtained from the mesocarp of the green coir *(Cocos nucifera* L.*)*. They are composed of cellulosic, hemicelluloses, pectin, tannins, polyphenols, flavonoids, and lignin as binding material [2]. Lignin and phytochemical components are widely used as corrosion inhibitors [3,4]. These macromolecules adsorb to the surface of the metallic substrate forming ferric compounds-macromolecules with the corrosion products, through a mixed inhibition mechanism [4,5].

In recent decades, there has been a lot of effort to provide eco-friendly and biodegradable materials [6–8]. Thus, many studies used agro-industrial waste in different sectors, including energy storage materials [9], thermoelectric materials [10], advanced ceramics [11,12], and composite materials. Soltani et al. [12] studied a freeze-casting route toward macroporous $SiOC/SiO_2$ ceramic nanocomposites from preceramic polymers. They used commercially available methylphenyl-vinyl-hydrogen polysiloxane and amorphous silica derived from rice husk ash freeze-dried with water or tert-butyl alcohol, cross-linked, and pyrolyzed at 1100 °C in nitrogen. The authors were successful in manufacturing polymer-derived macroporous amorphous $SiOC/SiO_2$ monoliths with aligned pore channels by freeze-casting techniques using water and tert-butyl alcohol as solvents. This result is evidence of the efficiency of reusing agricultural residues such as rice husk with raw material. Composite materials reinforced with natural fiber have also received continuous attention due to their wide application. Natural fibers have properties better than synthetic ones, such as low cost, low density, biodegradability, renewability, and considerable mechanical performance. In addition, the increase in the use of natural materials has led to a reduction in greenhouse gas emissions [13–15]. Sadeq et al. [2] used coconut fibers in their studies with different grain sizes ranging between 250 and 950 μm. The fibers were chemically treated with an alkaline solution and used as a reinforced agent for epoxy resin. Morphology and mechanical performance represented by impact and flexural strength to the pure polymer and the resulting composites were investigated. The results obtained confirmed a mechanical improvement for the composites compared to pure polymer.

Over the last few decades, organic coatings have been widely applied to protect metals [16]. The coatings industry is consolidated and has undergone a continuous change in technology in recent decades, mainly due to environmental factors, reducing the high toxicity of anticorrosive pigments incorporated in paints, such as chromium ions inhibitors [17]. Thus, the development of new components to improve the performance of these coatings is essential to further consolidate this industry.

Due to the potential of coconut fiber as a corrosion inhibitor and a large number of works in the literature as biocomposites incorporated with coconut fiber [13,14,18–20], combined with the search of non-toxic pigments in the industry, this work aims to characterize coconut microfibers for use as pigments for organic coatings. Thus, a novelty of this study is the characterization of the coconut fiber as an environmentally friendly inhibitor pigment for organic coatings.

## 2. Materials and methods

### 2.1. Materials

The mild steel was mechanically press-cut into samples of 1.7 cm × 4 cm (area = 6.8 $cm^2$) dimensions, for weight loss measurements and 4 cm × 4 cm for electrochemical measurements. The samples of the mild steel were ground with different grades (# 80,100, 240, 320, 400, 600, 800) silicon carbide paper, degreased in acetone (boiling point = 56 °C; polarity index = 5.1 and density = 0.791 g/mL at 20 °C), dried in warm air and stored in moisture-free desiccators prior to use. The aggressive medium was 3.5% (w/w) sodium chloride (NaCl) prepared from 98% analytical. The solution treatment alkaline was 5% (w/w) sodium hydroxide (NaOH) prepared from 98% analytical. Distilled water was used for the preparation of all reagents. The oil absorption tests used raw linseed oil with an acidity index of 1–3. The coconut fibers used in this study were donated by the Environment and Materials Laboratory – LAMM of the Department of Science and Technology of the State University of Santa Cruz – UESC, Ilhéus - BA.

### 2.2. Preparation of coconut fiber

First, the coconut fibers were comminuted in a pan mill, located in the Ore Treatment laboratory, Department of Metallurgical and Materials Engineering - DEMET, School of Engineering, Federal University of Minas Gerais - UFMG. After being comminuted, aiming at homogenization of the particle size, the fibers were sieved using a MESH 250 sieve, equivalent to 63 μm aperture.

### 2.3. Alkaline coconut fiber treatment

After the single sieving operation, part of the microfiber was subjected to a 24-h immersion alkaline treatment. The alkaline treatment of the fiber was carried out with a solution of sodium hydroxide (NaOH) P.A, at 5% (w/w). Subsequently, they were filtered with a vacuum pump using a qualitative filter paper and dried in an oven at 60 °C, for 4-h.

### 2.4. Coconut fiber characterization

Oil absorption tests were performed on the untreated (UM) and treated (TM) coconut fiber samples. In this experiment, 5 g of each sample was carefully weighted and each sample was placed in a Petri dish. With the aid of a graduated burette, the linseed oil was added drop by drop in each Petri dish. With the aid of the spatula, the pigment was mixed in the oil after the addition of each drop of oil. Further, the tests were completed when a thin, homogeneous, non-brittle paste without excess oil was obtained. At the end of the procedure, the spent volume

of linseed oil was determined, multiplied by its specific mass, so that the added oil mass was determined. Thus, through Eq. (1), the oil absorption of the studied samples was obtained.

$$Oil\ absorption = \frac{w_1\ x\ 100}{w_2} \quad (1)$$

where, $w_1$ = oil weight; $w_2$ = pigment weight.

The CPVC is the critical point, in the concentration of pigments and fillers, it is the minimum amount of polymer sufficient to fill the spaces between the particles [21,22]. In the study, the relationship between oil absorption (OA) and density ($\rho$) of assessments for CPVC determination (Eq. (2)).

$$CPVC = \frac{1}{\left(1 + \frac{(OA)(\rho)}{93,5}\right)} \quad (2)$$

Size distribution by laser diffraction was performed for the untreated (FN) and treated (FT) coconut microfiber samples, using Malvern Mastersizer 3000 equipment. First, coconut fibers were dispersed in water and placed in an ultrasom in order to guarantee the total fibers dispersion. After, the coconut fibers solution was analyzed, determining size distribution by volume.

The morphology of untreated and treated ground coconut fibers was evaluated by scanning electron microscopy - SEM. The equipment used was Tescan model Vega 3 LMU. Secondary electrons images (SE) were obtained using an acceleration voltage of 10kv, in different magnitudes values, with tungsten filament as a cathode.

The samples of coconut microfibers (FN) and (FT) was characterized by the FTIR-ATR technique. The FTIR-ATR analysis was performed on Bruker equipment, model Alpha II associated with OPUS software. Scanning wavelength was performed from 4000 to 500 $cm^{-1}$, in ATR mode.

Thermogravimetric analyzes (TG) were performed for the coconut microfiber samples using Netzsch equipment, model STA 449 F3 Jupiter, assisted by Proteus software. For the analysis, ~20 mg of sample was weighted in the crucible and later added to the equipment. The test was carried out in a nitrogen atmosphere ($N_2$), with a temperature range from 30 to 800 °C and a heating rate of 10 K/min.

The characterization size distribution by laser diffraction, SEM, FTIR and TG characterization was performed in the Electrochemistry and Corrosion Laboratory of the Polytechnic School of the University of São Paulo – USP.

Weight loss tests were performed in accordance with ASTM G31 – 72 (2017) Standard Guide for Laboratory Immersion Corrosion Testing of Metals. The carbon steel samples were carefully weighted on an analytical balance and completely immersed in 200 mL of solution in a 250 mL Erlenmeyer flask. The carbon steel weight loss tests were performed in a 3.5% (w/w) NaCl solution, with immersion for 720 h at room temperature (~25°). The tests were performed for control samples and with the incorporation of 5% (w/w) untreated (UM) and treated (TM) coconut microfiber, a triplicate of each condition. From the weight loss, it was possible to calculate the corrosion rate, through Eq. (3). The inhibition efficiencies of coconut microfiber samples can be calculated by Eq. (4).

$$C_R = \frac{w_1 - w_2}{At} \quad (3)$$

$$\eta_w(\%) = \frac{C_{R(controlsample)} - C_{R(inhibitor)}}{C_{R(controlsample)}}\ x\ 100 \quad (4)$$

where, $w_1$ = initial weight sample; $w_2$ = final weight sample; $C_R$ = corrosion rate; $A$ = sample area; t = immersion time; $\eta_w(\%)$ = inhibition efficiencies.

Potentiodynamic polarization tests were performed to characterize the corrosive inhibitory properties of the fiber samples. The tests were carried out using an Autolab 302 N potentiostat, in a three-electrode flatcell, with carbon steel as the working electrode with an exposed area of 1.2 $cm^2$, saturated calomel electrode (SCE) as a reference electrode, and a platinum wire as a counter electrode. Potentiodynamic polarization curves were obtained by scanning the electrode potential at a sweep rate of 0.167 V/s, with potential limits of ±2.5 mV vs OCP, in a 3.5 (w/w) NaCl electrolyte at 25 °C. The potentiodynamic tests were performed for the control sample and with the incorporation of 5% by mass of untreated (UM) and treated (TM) coconut microfiber. The samples were immersed for 2 h to stabilize the corrosion potential.

## 3. Results and discussion

### 3.1. Microfiber coir characterization

#### 3.1.1. Physical properties

The studied powder coconut fiber samples were characterized by their physical properties. These properties are important for its application, mainly as a pigment. The densities of untreated (UM) and treated (TM) powder coir fiber samples were measured; the observed values are 1.41 g/$cm^3$ for sample (UM) and 1.03 g/$cm^3$ for sample (TM) (Table 1). Adeniyi et al. [19] carried out a literature review study on the properties of coconut fiber. according to previous studies, the density values of coconut fiber are in the range of 1.1–1.5 g/$cm^3$. Authors Kumar and Raja [23], also searched for data in the literature and found a range of density values 1.45–2.8 g/$cm^3$. It can be seen in Table 1 that the density value found for the UM sample is within the range proposed by Adeniyi et al. [19], and slightly below the range portrayed by the authors Kumar and Raja [23]. The treated powder coconut fiber (TM) showed a lower value than the proposed intervals. This characteristic may be related to the effects provided by the chemical surface treatment, such as the removal of different impurities, oil, wax,

**Table 1 – Physical Proprieties powder coconut fiber.**

| Proprieties | Coir fiber (UM) | Treatment coir fiber(TM) |
|---|---|---|
| Density (g/$cm^3$) | 1.4 | 1.0 |
| Oil absorption (g/100g) | 95.7 | 99.5 |
| CPVC | 40.9 | 47.7 |
| Average size of particles (μm) | 9.2 ± 16.9 | 15.2 ± 21.9 |

and fats. In addition to the decrease in the content of materials such as cellulose and hemicellulose [14].

The low density is an advantage for a pigment because pigments work by volume but are sold by weight. Thus, considering the cost, a high-density pigment contains fewer particles per unit cost. Regarding its use as a filler, considering a control volume, a pigment with a lower specific mass has more particles per volume. However, the low specific mass of the particles can increase the agglomeration of particles [21,22]. According to Jones; Nichols and Pappas [24], the pigment density influences its oil absorption value, as pigments with higher density require less oil adsorbed on the surface, consequently, they have lower oil absorption. We can observe that the studied samples presented this behavior, inversely proportional values, about density and oil absorption.

The oil absorption was analyzed for the UM and TM samples, high values for oil absorption are observed, mainly the value presented by the treated coconut fiber (TM). The authors Przywecka [25] studied aluminum phosphate pigments modified with ammonia, calcium, and molybdenum. They obtained similar results for oil absorption, compared to the present study. The products were characterized by a high oil absorption number in the range of 97–127 g/100 g of product. The authors associated this behavior was with the presence of the amorphous phase in these pigments.

Oil absorption values can vary greatly according to the properties of each pigment. This physical property is related to the amount of binder sufficient to adsorb all the pigment particles [24] To achieve optimization in terms of formulation, both technically and in terms of cost, it is important to achieve the highest packing density of the mixture. This packing is obtained when a high distribution of particles is obtained, thus achieving an increase in CPVC [21]. According to [22] nontoxic organic pigments have a lower specific mass and greater oil absorption, increasing the possibility of formulating coatings that CPVC exceed PVC.

In this study, was observed a difference in the CPVC values of UM and TM. This difference is related to the sample properties: density and oil absorption. With these CPVC values obtained, it is possible to search an ideal PVC value for the samples of new pigments understudy, obtaining a formulation for the desired conditions. An important factor when considering PVC for the formulation is that due to the high oil absorption of the UM and TM powder coconut fiber samples, its use in the formulations must be at low levels [21].

### 3.1.2. *Powder size distribution by laser diffraction*

To determine the size distribution of the processed powder coir fiber particles, a laser diffraction analysis of the samples under study was performed. Fig. 1 shows the particle size distribution histogram and the curve of the accumulated values of the untreated coconut fiber sample. The particles had a powder size range from 0.40 μm to 127 μm, with the largest population, about 90% of the particles, being in a size range from 0.77 μm to 60 μm. The calculated mean particle size was 9.16 μm (Table 1).

Fig. 2 represents the particle size distribution histogram of the treated powder coir fiber. The particles had a size range from 0.40 μm to 111 μm, with the largest population, about 85%

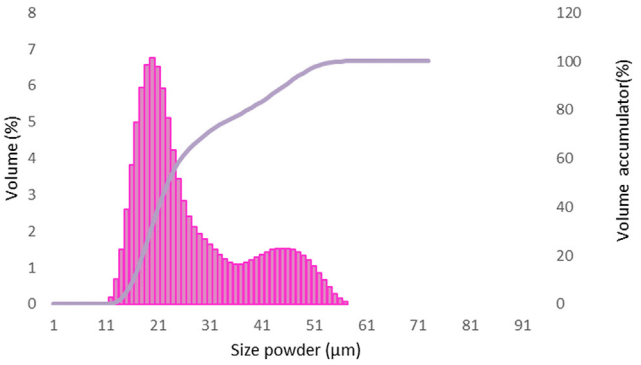


**Fig. 1 – Powder size distribution of untreated coconut fiber (UM).**

of the particles, being in a size range from 0.7 μm to 60 μm. The calculated average particle size was 15.26 μm (Table 1). As mentioned by Furtado [26], the solid's particle size is one of its intrinsic properties related to its performance as a pigment, a material with small particles is expected for application as a pigment. This property is directly influenced by the beneficiation (milling) process. Regarding the results obtained for the powder size distribution, it is observed that the material milling step was efficient, with the largest population of particles being in a small size range, obtaining a finely divided material. Above all, it is noted from the range of sizes obtained in the analysis that there was an agglomeration of particles, as the sieve used has a MESH 250, equivalent to 63 μm, consequently, the particles could not be larger than this. value. But these values of agglomerated particles were approximately 10% for UM and 15% for TM, just a small part of the total amount.

Comparing the size distribution of the samples, it is noted that the largest populations of untreated coconut fiber particles have a smaller size, we can observe this behavior in the histogram curve (Fig. 1) which shows a bimodal distribution. The first curve of the untreated coconut fiber (UM) particle size histogram vs. volume has ~80% of the particles. Observing Fig. 2, the largest populations of particles of treated coconut fiber (TM) also have a smaller size, represented by the first peak of the histogram particle size of the treated fiber (TM) vs. volume. However, it is noted that this value is less significant,

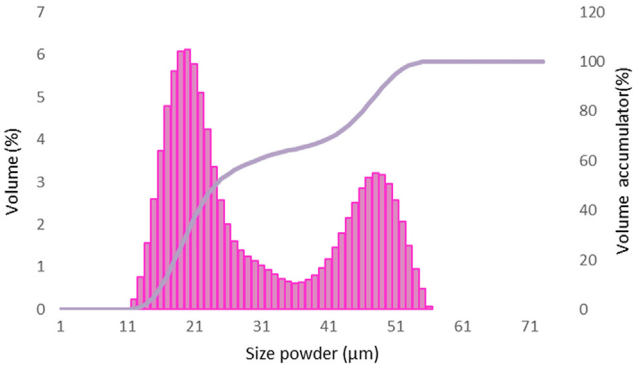


**Fig. 2 – Powder size distribution of treated coconut fiber (TM).**

compared with the results for untreated coconut fiber (UM). The first curve of the treated coconut fiber (TM) particle size histogram vs. volume, contains approximately ~70% of the particles. Thus, the UM sample presented, for the most part, smaller particles. This fact can be proven by the average values of particle sizes in Table 1. The average size of pigment particles is related to the symmetry of the distribution of particles by the coating, and the more asymmetric the greater the average particle size [21].

This size difference may be related to the higher probability of agglomeration in the particles of the treated fiber sample (TM), due to its lower specific mass. The particle's agglomeration state for a pigment is a key factor for its application, related to dispersibility factors. Factors such as strong agglomeration of particles can compromise good fluidity and cause irregularities in the barrier formed by the coating, forming free resin [21].

### 3.1.3. *Scanning electron microscopy - SEM*

According to Furtado [26], the shape of the particles is another important property of solids for their use as a pigment. Thus, Fig. 3 shows the secondary electrons images obtained by SEM of powder coir fiber in the different conditions studied, (a,b) untreated - UM; (c,d) treated - TM, respectively. It was observed for both samples, predominantly, lamellar-shaped particles, but there is the formation of some particles and needle-shaped agglomerates.

The extenders and lamellar pigments reinforce the structure of the film, reducing the tendency to crack and interruption of the film's continuity during its aging. They improve the impermeability and applicability of the coating, for example, paints with high corrosion resistance, with protection by a barrier mechanism, are formulated with lamellar pigments, so they can be applied in high thickness, providing durability in aggressive environments [21]. Pigments or extenders, depending on their acicular shape, reinforce the structure of the film, improve cohesion, improve abrasion resistance and flexibility [21].

Fig. 3(a,b) shows the SEM microscopy of powder coconut fiber UM, in which a material with a smooth surface is observed, in a matrix with embedded cells. According to Hasan et al. [14], this characteristic may be related to the

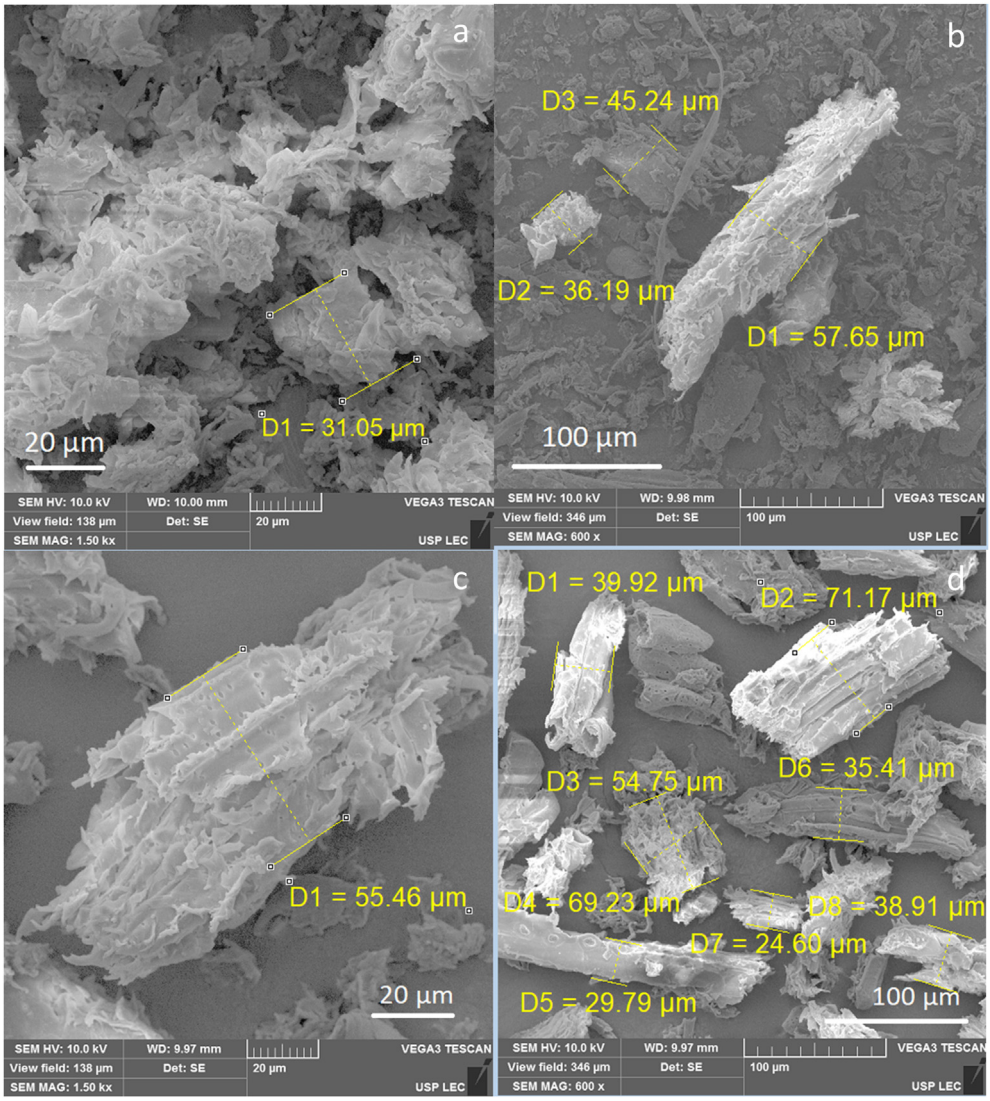


**Fig. 3 – Powder Coconut fiber images: (a,b) untreated coconut fiber (c,d) treated coconut fiber.**

presence of impurities on its surface, such as waxes and fatty acids, in addition to the fact that the coconut fiber cells are crystalline celluloses, arranged in a helical manner in an amorphous matrix, consisting of a cellulose-lignin complex. However, despite this lignocellulosic matrix, a porous surface is observed. Fig. 3(c,d) shows the SEM micrographs of powder coconut fiber with alkaline chemical treatment (TM). The TM surface micrograph is rough and exposed the microfibrils due to the removal of fatty acids, wax, globular particles, cuticle, and some part of hemicellulose and lignin [27]. An anisotropic surface is observed, with acicular shapes, where the arrangement of cellulose fibers that were inside the matrix is seen in the image. This material property can positively influence the application of the treated fiber.

The characteristics of treated coconut fiber may be related to the removal of cementing materials (lignin and hemicellulose) from the surface, in addition to the removal of fatty acids and waxes. According to Hasan [14], alkaline reagents such as aqueous NaOH solutions help natural fibers to ionize –OH groups. The degree of polymerization, molecular orientation, and chemical composition are all affected by alkaline treatments. Gholampour and Ozbakkaloglu [6] mention that the alkaline chemical treatment promotes the rupture of the lignin–cellulose–hemicellulose complex, as well as the removal of each of these fractions, consequently increasing the porosity of the material.

According to AdeniyI et al. [19], alkaline treatment can also lead to the decomposition of crystalline cellulose, which leads to the exposure of short crystallites, in addition to generating an increase in amorphous cellulose. We can see that the results were similar to those found in the literature, where the surface treatment with alkali is rougher, which may increase the wettability of the fiber, allowing a promising interaction with the epoxy resin.

Comparing with the particle size distribution by laser diffraction tests, we noticed from the images that the particles of both, treated coconut powder (TM) and untreated coconut powder (UM), have diameter values in almost all measures in agreement and very similar with the results obtained in the laser diffraction technique. It is importance to realize that the particle size by laser diffraction were made using sample solutions, as described in methodology, wich justifies a more dispersive system and also less particle size values compared with the SEM results, that are more likely to be shown with agglomeration tendency.

Another analogy is with the oil absorption value, we note that the sample with the most porous surface, despite having a larger particle size, presents greater oil absorption. This fact is to the detriment of the need to fill all these interstices.

### 3.1.4. *Fourier transform infrared spectroscopy - FTIR*

Fourier transform infrared spectroscopy analyzes were performed to characterize the samples referring to absorption peaks, before and after the alkaline treatment (NaOH). This characterization is necessary to analyze the chemical bonds and understand the behavior of the samples as a pigment. Fig. 4, shows the spectra of samples untreated powder coconut fiber (UM) and treated powder coconut fiber (TM).

The transmittance band of 3340 $cm^{-1}$, in the region 3500 $cm^{-1}$ - 3000 $cm^{-1}$, represents the OH stretching vibration,

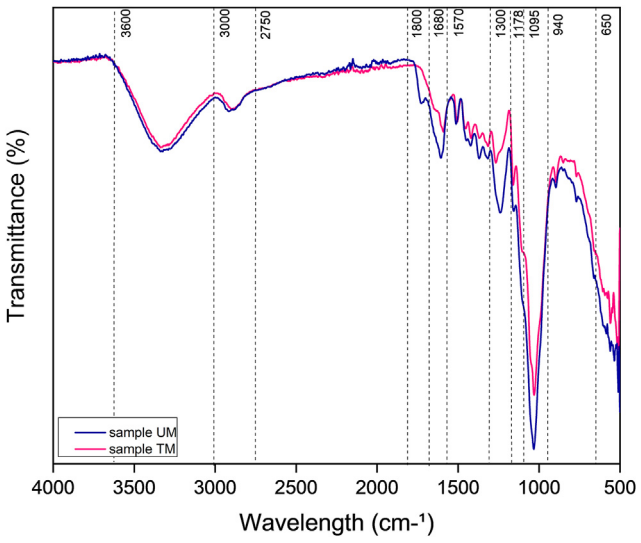


**Fig. 4 – Fourier transform infrared spectrum of coconut powder samples.**

a typical characteristic of natural fibers, due to the presence of the hydroxyl group present in cellulose and hemicellulose [27]. This band is found in the tannin and polyphenol spectra, due to hydroxyl-rich structures present in the aromatic rings [28]. The vibration peak near 2920 $cm^{-1}$ corresponds to the symmetrical vibration of C– H, which is related to the methylene and methyl groups. The aliphatic portions of hemicellulose and cellulose are indicated by these bands [14].

The peak in the region of 1730 $cm^{-1}$ was observed in the case of untreated fibers (UM), referring to the presence of C=O, present in hemicellulose, tannins, pectin, and wax, or carboxylic group of coumaric and ferulic acids of lignin. But note that the peak corresponding to this vibration disappeared in the sample with chemical treatment. This behavior indicates that the chemical treatment significantly removed hemicellulose, pectin, tannins, and waxes from the fiber surface [27]. The presence of the C=C bond is reflected by the peak at 1605 $cm^{-1}$, present in the aromatic rings. This vibration indicates a high number of interflavonoid bonds [4,28,29].

The peak around 1368 $cm^{-1}$, which belongs to the –CH– of cellulose and hemicellulose, almost disappeared after the alkaline treatment, because the NaOH treatment removed part of the hemicellulose components from the fiber. The peak in the 1240 $cm^{-1}$ region reflects the C–O stretching acetyl group on the lignin and shows a significant reduction. This reduction is attributed to the degradation of lignin after chemical treatment. The peak around 1156 $cm^{-1}$, which corresponds to the C–O–C elongation of the polysaccharide components of cellulose, showed a significant reduction after chemical treatment. This reduction is due to the degradation of the cellulose components of the fiber. The absorption peak around 1032 $cm^{-1}$ corresponds to both CO elongations in cellulose, hemicellulose, and lignin, and CO–C elongation in hemicellulose and cellulose and was observed to be more prominent for sample UM [27].

Through the FTIR results, the progression of the maceration process results in the deterioration of the content of the main components of the lignocellulosic complex. Chemical treatment

generated the rupture of the lignin–cellulose–hemicellulose complex, as well as the removal of each of these fractions through delignification pre-treatment techniques, in which the removal of lignin and hemicellulose promotes the reduction of cellulose crystallinity and, consequently, increased porosity of the material [6].

According to Santos et al. [30], cellulose is amphiphilic, part hydrophobic, and part hydrophilic. Thus, cellulose favors the linear growth of the chain, confering insolubility in water, a considerable degree of crystallinity, high molecular weight, and rigid structure. The complex formed of cellulose/hemicellulose gives rigidity to the cell walls, this property of these chemical components can be interesting to confer mechanical properties to the coating, in the application as extenders. This component presented in coconut fiber could also help in its application as a pigment or extenders, as it gives the material greater hydrophobicity. Gallindo et al. [31], analyzed the moisture content of fibers with and without alkaline treatment, the moisture content found was 5% for the untreated fiber and 18% for the treated fiber. Although the alkaline treatment increases the cellulose composition, to the detriment of hemicellulose decomposition, this increase is amorphous cellulose, making the treated coconut fiber material more hydrophilic [19,32–35].

Lignin is an amorphous polyphenolic material, alkaline hydrolysis assists in the solubilization and extraction of the lignin present in the biomass, increasing the internal surface and decreasing the degree of polymerization [5]. Although lignin hydrolysis occurs, consecutively, hemicellulose degradation occurs and, generally, in a more significant way. Thus, hemicellulose and lignin, which are found in the surface layer of the fibers, are hydrolyzed. However, there is a significant amount of lignin in the innermost layer of the fiber, known as the cellulose-lignin matrix. of coconut [4].

This alkaline hydrolysis process may be interesting for the application of coconut fiber powder as a pigment, as lignin and unmodified lignin monomers show great potential as corrosion inhibitors in acidic, basic, and neutral media [3]. The authors Ding et al. [36] proved this synergistic effect of lignin, they analyzed the feasibility of incorporating epoxidized lignin, as an additive in coatings, based on epoxy resin for anticorrosive purposes. The modification by epoxidation of lignin was carried out using epichlorohydrin (EGL) under alkaline conditions. The anticorrosive properties of ELG/epoxy coatings on carbon steel immersed in 3.5% (w/w) NaCl solution were studied by polarization curves and electrochemical impedance spectroscopy (EIE). Compared with pure epoxy coating, the addition of ELG greatly improved the corrosion protection performance of the steel. Epoxy coating with 2% ELG, achieved high corrosion protection performance.

Condensed tannin consists of four flavonoid monomers, such as catechin, epicatechin, epigallocatechin, and epicatechin gallate [29]. According to Umoren et al. [4], we found other chemical phytocomponents present in coconut fiber. These molecules may aid in the synergistic effect to inhibit corrosion. Studies were carried out with treated tannin from Rhizopora mucronata (RMT) as a corrosion inhibitor for carbon steel and copper. The corrosion rate of carbon steel and copper in 3% NaCl solution was studied using the weight loss technique and electrochemical studies. The inhibitory efficiency of RMT was compared with the commercial inhibitor sodium benzotriazole (S- BTA). The best concentration of RMT was 20% (m/v), increasing the concentration of RMT decreased the corrosion rate and increased the inhibitory efficiency. The trend of RMT was similar to that of BTA-S, but its inhibitory efficiency for carbon steel was poor (6%) compared to RMT (59%). BTA-S was efficient for copper (76%) compared to RMT (74%). RMT was efficient even at low concentrations, therefore, the use of RMT as an economical and environmentally friendly corrosion inhibitor for carbon steel is feasible. The corrosion inhibitory effect of RMT was attributed by the authors to the presence of flavonoid monomers. These monomers can react with newly generated $Fe^{2+}$ ions on the corroding metallic surface, resulting in the formation of organometallic complexes [29]. Therefore, the presence of tannins and other phytochemical constituents in coconut fiber presents the potential for its application as a corrosion-inhibiting pigment. However, the alkaline treatment can extract these components, consequently, it can be harmful for its use as an inhibitor pigment.

### 3.1.5. *Thermogravimetric analysis*

To understand the thermal behavior of coconut fiber, samples, untreated (UM) and treated (TM), were subjected to thermogravimetric analysis. Untreated and treated fiber TG and DTG curves are shown in Figs. 5 and 6, respectively. Thermogravimetric analysis (TG) is a useful method to investigate the mass loss of materials [14]. The TG curves of the samples show different mass loss processes. The UM samples underwent four-stage degradation processes (Fig. 5). However, the TM sample shows degradation processes in three stages (Fig. 6).

The thermal degradation of lignocellulosic fiber is mainly due to the degradation of hemicellulose, cellulose, and lignin. Due to the acetyl groups in its composition, hemicellulose has lower thermal stability than cellulose and lignin [37]. Among these components, lignin has greater thermal stability, due to its complex structure with aromatic groups, its degradation occurs over a wide temperature range [27]. The first mass loss process for the UM sample was observed between 30 and 127 °C, approximately 9.32% mass loss. For the TM sample, the

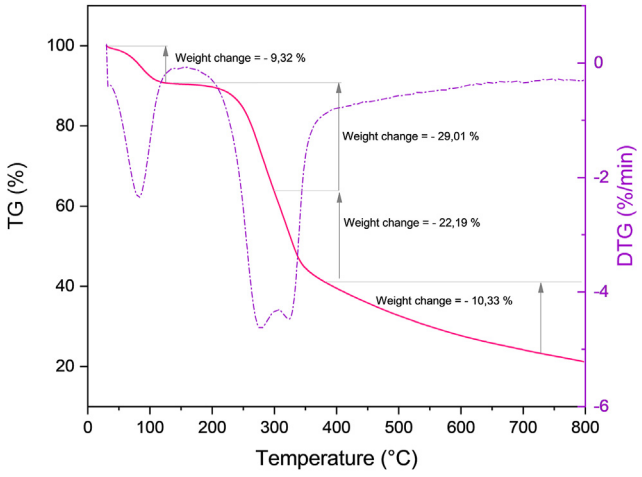


**Fig. 5 – Thermogravimetric analysis untreated coconut fiber (UM).**

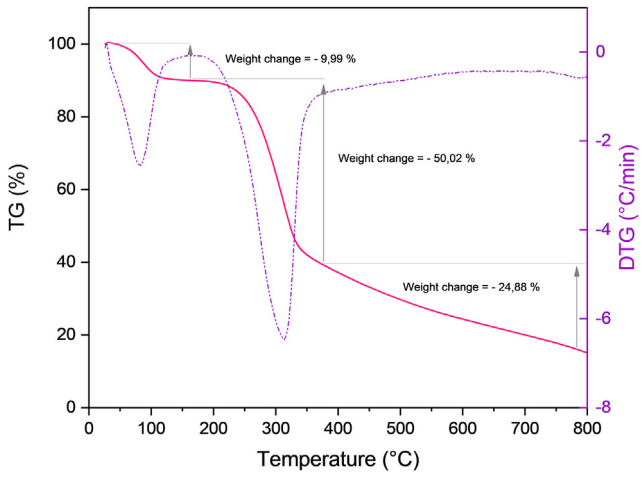


**Fig. 6 – Thermogravimetric analysis treated coconut fiber (TM).**

mass loss was in the range of 30–160 °C (~9.99% mass loss). This process is associated with the loss of moisture from the material [14]. In this second degradation process, we observed the difference between the behavior of the samples. The UM sample showed mass loss over the temperature range 127–300 °C (~29.01% mass loss).

The authors Prasad et al. [14], performed thermogravimetric (TG) analyses for coconut fiber and associated the loss of mass in this temperature range with the decomposition of hemicellulose, pectin, cleavage of the glycosidic bond of cellulose, and part of the lignin. The TM sample, on the other hand, presented a different behavior, as the sample presented only 3 stages of decomposition, the second process of mass loss was in a temperature range of 160–360 °C, with approximately 50.02% of mass loss. This is the main process of mass loss for treated fiber, attributed to the decomposition of cellulose by breaking glycosidic bonds of the glucose chain and decomposition of lignin, but to a lesser extent [14].

This different behavior between the samples corroborates the results obtained by FTIR analysis, which revealed the disappearance of the associated C = O band for the treated fiber. Thus, it indicates that the chemical treatment significantly removed hemicellulose, pectin, and part of the lignin. The behavior of the samples in the thermogravimetric analysis can be confirmed by the derivative thermogravimetric analysis curves (DTG), where we can observe a peak at approximately 280 °C for the untreated fiber. This peak is not observed for the treated coconut fiber sample. The third mass loss process for the untreated coconut fiber (UM) sample, temperature range 300–400 °C, is attributed to the decomposition of cellulose by breaking the glycosidic bonds of the glucose chain and decomposition, in a lower percentage., from lignin [14].

From the DTG curves, the derivative peak associated with the maximum rate of mass loss is observed around 280 °C (~29.01% mass loss) for UM and, 315 °C (mass loss ~50.02%) for TM. The lower degradation of the untreated fiber observed is related to the presence of hemicellulose and pectin in its composition, which exhibits low thermal stability, while the treated fiber is more stable due to the removal of these components [14,27].

The last process, the fourth step for the UM sample and the third step for the TM sample, associated with the mass loss of mass above 380 °C, corresponds for the two samples to the degradation of the remaining lignin and the oxidative decomposition of the carbonized residue [14].

The thermal characterization of the material is important to understand its behavior and to analyze the possibilities of thermal treatments for its incorporation as a pigment. Considering the application as an inhibitory pigment, with a lignin inhibition mechanism, the ideal treatment temperature would be 280 °C for UM and 315 °C for TM. At this temperature, it is possible to purify the lignin present in the samples, due to its greater thermal stability, but as a consequence, it could increase its hydrophilicity [27]. Considering the application as a filler or inhibitory pigment related to tannins, the ideal heat treatment would be at 120 °C for UM and 160 °C for TM, removing only the moisture from these materials. Regarding the application as extenders, structuring materials such as cellulose/hemicellulose/lignin may be interesting to improve the mechanical properties of materials [14]. On the other hand, considering applying as an inhibitory pigment referring to the tannin inhibition mechanism, we have that the removal of these materials at high temperatures can be harmful [3].

### 3.2. *Gravimetric tests - mass loss measurements*

The weight loss tests were performed for carbon steel samples, immersed in 3.5% NaCl and NaCl 3.5% with 5% by mass of untreated (UM) and treated (TM) coconut microfiber. Table 2 shows the results obtained in the gravimetric tests, for the tested condition. The corrosion rate for the carbon steel control sample was considerably higher, compared to samples with microfiber incorporation in the medium, both untreated sample (UM) and treated sample (TM). Among the test conditions, the one that presented the best performance was the treated coconut microfiber, with an inhibition efficiency of ~90%.

Where the coconut fiber samples showed high corrosion inhibition efficiencies and, in image 7 one can observe the physical aspect of the samples (triplicate of each condition), after the mass loss tests. Note that for the samples with untreated coconut microfiber (UM) and the control sample, the type of corrosion was generalized (Fig. 7).

However, for samples immersed in a solution with a treated coconut fiber sample (TM) (Fig. 7), corrosion was localized, characterized by pitting. It can be seen that the pits were formed mainly in the regions where the carbon steel pieces were tied with nylon and at the ends of the samples. The lower corrosion rate of the coconut fiber treated as an inhibitor may be related to the higher lignin content in the coconut microfiber, due to the alkaline treatment. In addition

**Table 2 – Weight loss test results.**

| Sample | Corrosion Rate $C_R$ (g/m$^2$.h) | Inhibitor efficiency $\eta_w$(%) |
|---|---|---|
| UM 5% (w/w) | 0.803 | 68.36 |
| TM 5% (w/w) | 0.275 | 89.28 |
| Control sample | 2.539 | – |

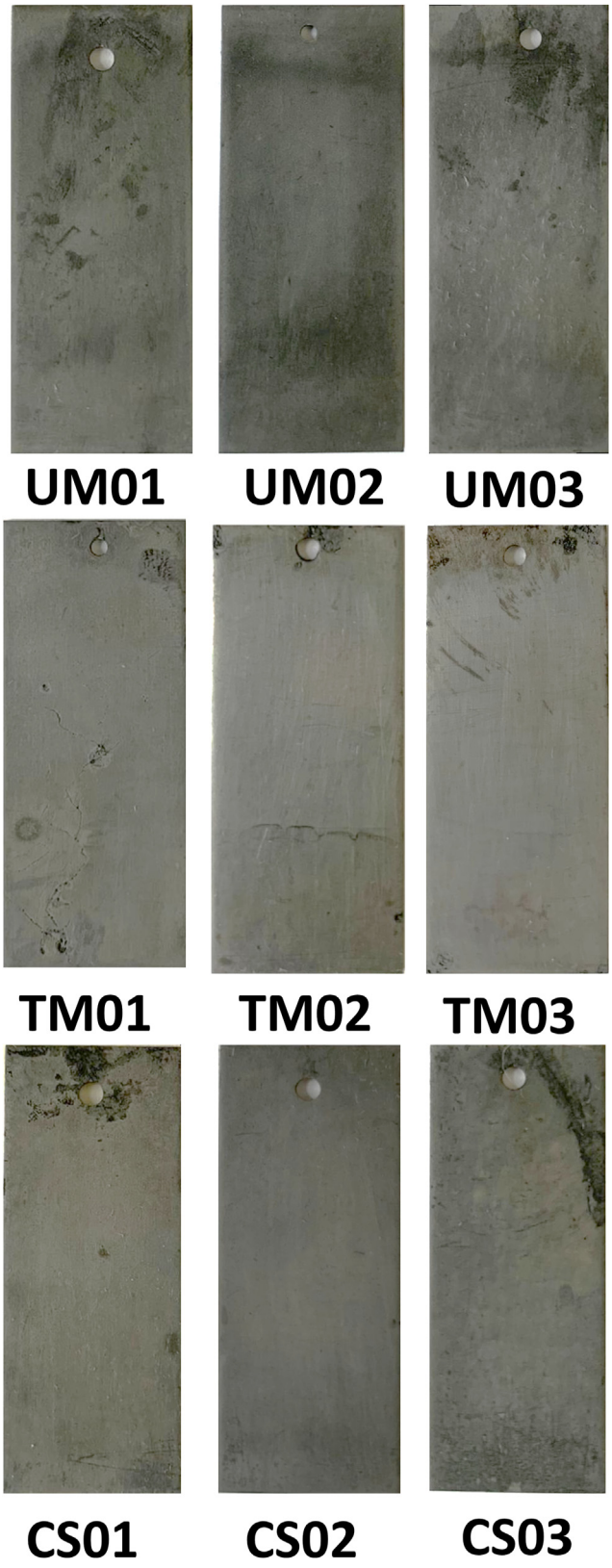


**Fig. 7 – Carbon steel samples immersed in 3.5% NaCl solution (UM – 5% (w/w) untreated powder coconut microfiber, TM – 5% (w/w) treated powder coconut microfiber, and CS – control sample).**

to the fact that the type of corrosion in carbon steel is localized, which causes less material loss, it is of extreme concern for plant safety, as it is difficult to control and can cause catastrophic damage.

### 3.3. *Potentiodynamic polarization tests*

Potentiodynamic polarization studies were carried out to evaluate the anticorrosive inhibition properties of coconut microfiber, with a concentration of 5% (w/w) in 3.5% (w/w) NaCl solution, on the carbon steel substrate. Fig. 8 shows the potentiodynamic polarization curves for untreated coconut microfiber (UM), treated coconut microfiber (TM), and control sample (blank). Analyzing the curves qualitatively, a shift of the anodic curves towards the most positive region, for sample treated powder coconut fiber (TM). This behavior indicates that the inhibitor has an anodic behavior.

When looking at the resulting corrosion current density values for the samples, mainly in the anodic branch, we can verify that the powder green coconut microfiber acts as a corrosion inhibitor for the carbon steel in NaCl 3.5% (w/w), since the UM and TM samples presented lower values than those presented by the control sample. The better performance of treated coconut fiber as an inhibitor may be related to the higher lignin content in TM coconut microfiber. Although this treatment removes part of all components of the coconut mesocarp, the material most resistant to this process is lignin, thus increasing its concentration [27]. To the untreated coconut fiber (UM) sample, this performance difference about the TM sample may be related to the higher percentage of hemicellulose on the surface, reducing the contact of photochemical components and lignin, however, compared to the sample in white, the UM coconut microfiber sample showed inhibition efficiency. Thus, the results found in the potentiodynamic polarization tests corroborate the results obtained in the mass loss test, the untreated (UM) and treated (TM) powder coconut microfiber showed potential for

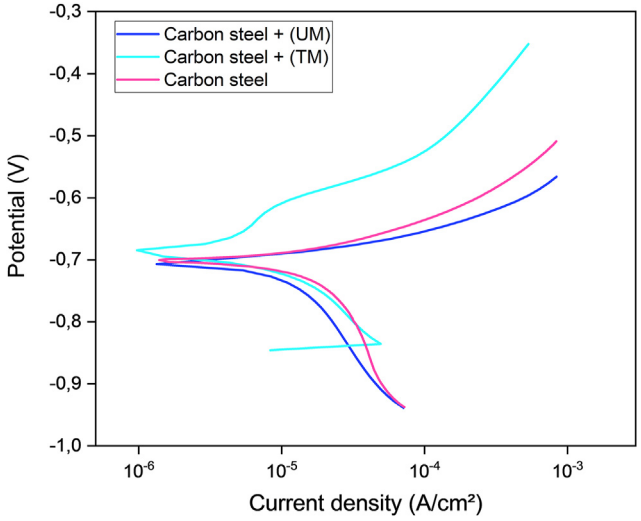


**Fig. 8 – Potentiodynamic polarization test curves.**

application as inhibitor pigments, due to their behavior as anti-corrosion inhibitors.

However, for the application of this powder material as a corrosion inhibitor, more careful studies are needed, such as optimization of the coconut fiber concentration and different temperatures. Despite the data reported in the literature using coconut fiber or husk as an efficient anti-corrosion inhibitor, the objective of the present study is only to verify this behavior of the material, to characterize and study the feasibility of application as an inhibitor pigment in anticorrosive organic coatings.

## 4. Conclusion

Coconut microfibers showed favorable properties for their application as an inhibitory pigment. Regarding its physical properties, the samples showed low density and high oil absorption for both untreated and alkali-treated samples, this fact may be that this behavior helps in coating with medium CPVC. However, pigments with high adsorption must be used in small percentages, making it difficult to apply as a filler pigment. The size distribution showed a finely divided material, with average particle sizes of 9.16 μm for UM and 15.26 μm for TM. This difference in particle size is due to the greater tendency of the treated sample to agglomerate, more visible in less dense materials. This characteristic can be disadvantageous for its application as a pigment because the tendency of agglomeration together with the high oil absorption generates free resin. The SEM images showed particles with predominantly lamellar-shaped and needle-shaped, these particle shapes are common in pigments. Through the SEM images, it was possible to analyze the difference between the surfaces of the material, it is noted that the treated samples, due to the chemical change generated by the alkaline treatment, presented an anisotropic surface, with a greater number of interstices, which may help in its application due to greater interaction with the coating resin.

The FTIR spectra confirm the components reported in the coconut fiber literature, in addition to proving the effect of degradation and chemical alteration of lignocellulosic components. Thermogravimetric analyses investigated the application of coconut microfiber, and it was found that the material presents thermal stability at low temperatures, mainly due to the lignin in its composition, and generates the possibility of thermal treatment in the material for the purification of more thermally stable components. The mass loss tests also showed an inhibitory effect of coconut microfiber, decreasing the corrosion rate, the inhibition efficiency achieved was ~70% for the untreated sample and ~90% for the treated sample. The potentiodynamic polarization tests generated a decrease in the current densities of the samples in the anodic branch, mainly in the TM sample proving its inhibitory effect. They can be classified as anodic inhibitor. The behavior of the curves demonstrates an anodic inhibition mechanism. Thus, the characterization of this coconut fiber powder shows potential as an inhibitory pigment. Some difficulties were presented for the execution of the methodology, but the main one was about the coconut microfiber filtering process, due to the low particle size, the filtering process was difficult, spending a lot of energy with the vacuum pump thus the best alternative would be to treat the material and then benefit from grinding. Another factor to be improved in the methodology is the mill used, despite the milling efficiency having been high and having obtained a finely divided material, the mill used has a very small capacity of grinding batch material, allowing the equipment to be damaged and still high energy expenditure.

## Declaration of Competing Interest

The authors declare that they have no known competing financial interests or personal relationships that could have appeared to influence the work reported in this paper.

## Acknowledgment

Acknowledgments to the Federal University of Minas Gerais – UFMG, especially to the Graduate Program in Chemical Engineering to support and structure. Great to the support of the Próreitoria de pesquisa (PRPq) of the Federal University of Minas Gerais.The present work is thankful to the students of the research group Labcor - Laboratory of Corrosion of the Department of Chemical Engineering for the exchange of knowledge and grateful to CNPq - scholarship (# 130588/2020-2, #140187/2017-0 and 310504/2020-1). Great to the Electrochemistry and Corrosion Laboratory of the Polytechnic School of the University of São Paulo – USP for the partnership and instrumental chemical analyses performed. Treatment Laboratory, Department of Metallurgical and Materials Engineering - DEMET, School of Engineering, Federal University of Minas Gerais - UFMG for the use of the pot mill equipment and also to the Environment and Materials Laboratory - LAMM of the Department of Science and Technology of Santa Cruz State University – UESC, Ilhéus-BA to donating the coconut fiber used in this study.

## REFERENCES

[1] FAO. Food and agriculture organization of the united nations. World Prod; 2019.
[2] Sadeq NS, Mohammadsalih ZG, Mohammed RH. Effect of grain size on the structure and properties of coir epoxy composites. SN Appl Sci 2020;2:1–9. https://doi.org/10.1007/s42452-020-2991-x.
[3] Carlos De Haro J, Magagnin L, Turri S, Griffini G. Lignin-based anticorrosion coatings for the protection of aluminum surfaces. ACS Sustainable Chem Eng 2019;7:6213–22. https://doi.org/10.1021/acssuschemeng.8b06568.
[4] Umoren SA, Solomon MM, Eduok UM, Obot IB, Israel AU. Inhibition of mild steel corrosion in H2SO4 solution by coconut coir dust extract obtained from different solvent systems and synergistic effect of iodide ions: ethanol and acetone extracts. J Environ Chem Eng 2014;2:1048–60. https://doi.org/10.1016/j.jece.2014.03.024.
[5] Dastpak A, Yliniemi K, Monteiro MC de O, Höhn S, Virtanen S, Lundström M, et al. From waste to valuable resource: lignin as a sustainable anti-corrosion coating. Coatings 2018;8. https://doi.org/10.3390/COATINGS8120454.

[6] Gholampour A, Ozbakkaloglu T. A review of natural fiber composites: properties, modification and processing techniques, characterization, applications. J Mater Sci 2020;55. https://doi.org/10.1007/s10853-019-03990-y. Springer US.
[7] Sahu P, Gupta MK. Lowering in water absorption capacity and mechanical degradation of sisal/epoxy composite by sodium bicarbonate treatment and PLA coating. Polym Compos 2020;41:668–81. https://doi.org/10.1002/pc.25397.
[8] Sood M, Dwivedi G. Effect of fiber treatment on flexural properties of natural fiber reinforced composites: a review. Egypt J Pet 2018;27:775–83. https://doi.org/10.1016/j.ejpe.2017.11.005.
[9] Soltani N, Bahrami A, Giebeler L, Gemming T, Mikhailova D. Progress and challenges in using sustainable carbon anodes in rechargeable metal-ion batteries. Prog Energy Combust Sci 2021;87:100929. https://doi.org/10.1016/j.pecs.2021.100929.
[10] Bahrami A, Schierning G, Nielsch K. Waste recycling in thermoelectric materials. Adv Energy Mater 2020;10. https://doi.org/10.1002/aenm.201904159.
[11] Bahrami A, Simon U, Soltani N, Zavareh S, Schmidt J, Pech-Canul MI, et al. Eco-fabrication of hierarchical porous silica monoliths by ice-templating of rice husk ash table ESI-1. Chemical composition (wt. %) and density of rice husk, ARHA and CRHA. Green Chem 2016:1–2.
[12] Soltani N, Simon U, Bahrami A, Wang X, Selve S, Epping JD, et al. Macroporous polymer-derived SiO2/SiOC monoliths freeze-cast from polysiloxane and amorphous silica derived from rice husk. J Eur Ceram Soc 2017;37:4809–20. https://doi.org/10.1016/j.jeurceramsoc.2017.06.023.
[13] Santos JC do, Oliveira LÁd, Gomes Vieira LM, Mano V, Freire RTS, Panzera TH. Eco-friendly sodium bicarbonate treatment and its effect on epoxy and polyester coir fibre composites. Construct Build Mater 2019;211:427–36. https://doi.org/10.1016/j.conbuildmat.2019.03.284.
[14] Hasan KMF, Horváth PG, Bak M, Alpár T. A state-of-the-art review on coir fiber-reinforced biocomposites. RSC Adv 2021;11:10548–71. https://doi.org/10.1039/d1ra00231g.
[15] Fiore V, Sanfilippo C, Calabrese L. Dynamic mechanical behavior analysis of flax/jute fiber-reinforced composites under salt-fog spray environment. Polymers 2020;12. https://doi.org/10.3390/polym12030716.
[16] Lyon SB, Bingham R, Mills DJ. Advances in corrosion protection by organic coatings: what we know and what we would like to know. Prog Org Coating 2017;102:2–7. https://doi.org/10.1016/j.porgcoat.2016.04.030.
[17] Ziganshina M, Stepin S, Karandashov S, Mendelson V. Complex oxides – non-toxic pigments for anticorrosive coatings. Anti-corrosion Methods & Mater 2020;67:395–405. https://doi.org/10.1108/ACMM-12-2019-2222.
[18] Walte AB, Bhole K, Gholave J. Mechanical characterization of coir fiber reinforced composite. Mater Today Proc 2020;24:557–66. https://doi.org/10.1016/j.matpr.2020.04.309.
[19] Adeniyi AG, Onifade DV, Ighalo JO, Adeoye AS. A review of coir fiber reinforced polymer composites. Compos B Eng 2019;176:107305. https://doi.org/10.1016/j.compositesb.2019.107305.
[20] Yan L, Chouw N, Huang L, Kasal B. Effect of alkali treatment on microstructure and mechanical properties of coir fibres, coir fibre reinforced-polymer composites and reinforced-cementitious composites. Construct Build Mater 2016;112:168–82. https://doi.org/10.1016/j.conbuildmat.2016.02.182.
[21] Fazenda JMR. Tintas-Ciência e Tecnologia. 4°. Blucher; 2009.
[22] Koleske J. Paint and coating testing manual. Google Libros; 2012.
[23] Kumar SS, Raja VM. Processing and determination of mechanical properties of Prosopis juliflora bark, banana and coconut fiber reinforced hybrid bio composites for an engineering field. Compos Sci Technol 2021;208:108695. https://doi.org/10.1016/j.compscitech.2021.108695.
[24] Jones FN, Nichols ME, Pappas SP. Organic coatings: science and technology. 4th ed. 2017.
[25] Przywecka K, Grzmil B, Kowalczyk K, Sreńscek-Nazzal J. Studies on preparation of phosphate pigments for application in composite protective coatings. Prog Org Coating 2018;119:44–9. https://doi.org/10.1016/j.porgcoat.2018.02.009.
[26] Furtado P. Pintura anticorrosiva dos metais. Rio de Janeiro: Livros Técnicos e Cientiífcos Editora S.A.; 2010.
[27] Prasad N, Agarwal VK, Sinha S. Thermal degradation of coir fiber reinforced low-density polyethylene composites. IEEE J Sel Top Quant Electron 2018;25:363–72. https://doi.org/10.1515/secm-2015-0422.
[28] Morbeck FL, Lelis RCC, Schueler MVE, Santos WA, Sampaio DA, Da Silva BC, et al. Extraction and evaluation of tannin from green coconut mesocarp. Rev Mater 2019;24. https://doi.org/10.1590/s1517-707620190003.0748.
[29] Agi A, Junin R, Rasol M, Gbadamosi A, Gunaji R. Treated Rhizophora mucronata tannin as a corrosion inhibitor in chloride solution. PLoS One 2018;13:1–19. https://doi.org/10.1371/journal.pone.0200595.
[30] dos Santos JC, Siqueira RL, Vieira LMG, Freire RTS, Mano V, Panzera TH. Effects of sodium carbonate on the performance of epoxy and polyester coir-reinforced composites. Polym Test 2018;67:533–44. https://doi.org/10.1016/j.polymertesting.2018.03.043.
[31] Gallindo A de AS, Lima EG, Barros SRRC, Rodrigues POG, Freire MG. Avaliação da composição da casca de coco verde in natura E pós-tratamento químico como biomassa. https://editorarealize.com.br/artigo/visualizar/64922; 2020.
[32] Abraham E, Deepa B, Pothen LA, Cintil J, Thomas S, John MJ, et al. Environmental friendly method for the extraction of coir fibre and isolation of nanofibre. Carbohydr Polym 2013;92:1477–83. https://doi.org/10.1016/j.carbpol.2012.10.056.
[33] Sharma S, Kumar A. Recent advances in metallic corrosion inhibition: a review. J Mol Liq 2021;322:114862. https://doi.org/10.1016/j.molliq.2020.114862.
[34] Saba N, Tahir PM, Jawaid M. A review on potentiality of nano filler/natural fiber filled polymer hybrid composites. Polymers 2014;6:2247–73. https://doi.org/10.3390/polym6082247.
[35] Mittal M, Chaudhary R. Experimental study on the water absorption and surface characteristics of alkali treated pineapple leaf fibre and coconut husk fibre. Int J Appl Eng Res 2018;13:12237–43.
[36] Ding J, Gu L, Dong W, Yu H. Epoxidation modification of renewable lignin to improve the corrosion performance of epoxy coating. Int J Electrochem Sci 2016;11:6256–65. https://doi.org/10.20964/2016.07.56.
[37] Shebani AN, van Reenen AJ, Meincken M. The effect of wood extractives on the thermal stability of different wood-LLDPE composites. Thermochim Acta 2009;481:52–6. https://doi.org/10.1016/j.tca.2008.10.008.